

Supporting Information

Self-Assembled Monolayer Epitope Bridges for Molecular Imprinting and Cancer Biomarker Sensing

Julia Drzazgowska, Bianca Schmid, Roderich Süssmuth and Zeynep Altintas*

Institute of Chemistry, Technical University of Berlin, Straße des 17. Juni 124, 10623 Berlin, Germany

*Corresponding author: Zeynep Altintas

zeynep.altintas@tu-berlin.de

Table of Contents

Table S1. Peptide synthesis and characterization.	S-3
Table S2. Experimental parameters used for all electrochemical protocols in PalmSens4 electrochemical workstation.....	S-3
Equation 1. Calculation of relative signal suppression (%).....	S-4
Equation 2. Calculation of dissociation constant.....	S-4
Figure S1. The comparative rebinding studies with the MIPs formed on gold wires or QCM crystals..	S-4
Figure S2. Optimization of template concentration.....	S-5
Figure S3. Optimization of template removal by applying three different anodic potentials.....	S-5
Figure S4. Optimization of template removal by applying three different cathodic potentials.....	S-6
Figure S5. Characterization of molecular imprinting process from bare electrode surface to the end of template removal.....	S-7
Figure S6. The AFM characterization of molecular imprinting process based on the 2D height images at 10 μm^2 scale.....	S-8
Figure S7. The AFM characterization of molecular imprinting process based on the 3D surface topology images at 10 μm^2 scale	S-9
Figure S8. The AFM characterization of molecular imprinting process based on the 2D height images at 3 μm^2 and 1 μm^2 scales	S-9
Figure S9. The AFM characterization of molecular imprinting process based on the 3D surface topology images at 3 μm^2 and 1 μm^2 scales	S-10
Figure S10. The SEM characterization of molecular imprinting process	S-11
Figure S11. The EDX spectrum of MIP before and after template removal	S-12
Figure S12. Square wave voltammograms showing the NSE biomarker detection in buffer using the MIP sensor.....	S-13
Figure S13. Concentration dependent peptide detection using the MIP sensor and affinity determination.....	S-13
Figure S14. Comparison of affinity binding between the MIP and the NIP	S-14
Figure S15. The Scatchard plot for affinity determination of the sensor for NSE protein in serum....	S-14

Table S1. Peptide synthesis and characterization. Gradient system for the different peptide variants with their ESI-HR-MS data. Flow-rate: 20 mL min⁻¹; UV-detection at $\lambda = 210$ nm; buffer A: 0.1% TFA in H₂O; buffer B: 0.1% TFA in methanol. *Purification by HPLC is not necessary.

Peptide	X/ %	Y/ %	ESI-HR-MS	
			<i>m/z</i> [M+2H] ²⁺ calculated	ESI-HR-MS <i>m/z</i> [M+2H] ²⁺ found
The target peptide*	-	-	549.30111	549.30167
The modified template	30	90	934.98969	934.98910

Table S2. Experimental parameters used for all electrochemical protocols in PalmSens4 electrochemical workstation.

Measurements			
Cyclic Voltammetry		Square Wave Voltammetry	
t equilibration [s]	2	t equilibration [s]	1
E begin [V]	0.8	E begin [V]	-0.3
E vertex1	0.8	E end [V]	0.8
E vertex 2	-0.2	E step [V]	0.003
E step [V]	0.004	Amplitude [V]	0.05
Scan rate [V/s]	0.1	Frequency [Hz]	10 or 5
Number of scans	3		
Polymerization		Template removal	
MultiStep Amperometry		MultiStep Amperometry	
t equilibration [s]	0	t equilibration [s]	2
t interval [s]	0.002	t interval [s]	0.002
cycles	25 or 50	cycles	1
levels	2	levels	1
E level 1 [V]	0	E level 1 [V] (applied potentials)	-1.2 -1.0 -0.8 +0.9 +1.2 +1.4
t 1 [s]	5	t 1 [s]	30
E level 2 [V]	0.9		
t 2 [s]	1		

Equation 1. Calculation of relative signal suppression (%).

$$\text{Signal supresion [\%]} = \left(\frac{\text{template removal}_{\text{peak current}} - \text{target binding}_{\text{peak current}}}{\text{template removal}_{\text{peak current}}} \right) * 100\%$$

Equation 2. Calculation of dissociation constant. (m= Slope of the Scatchard plot; K_d = dissociation constant)

$$m = -\frac{1}{K_d}$$

$$K_d = -\frac{1}{m}$$

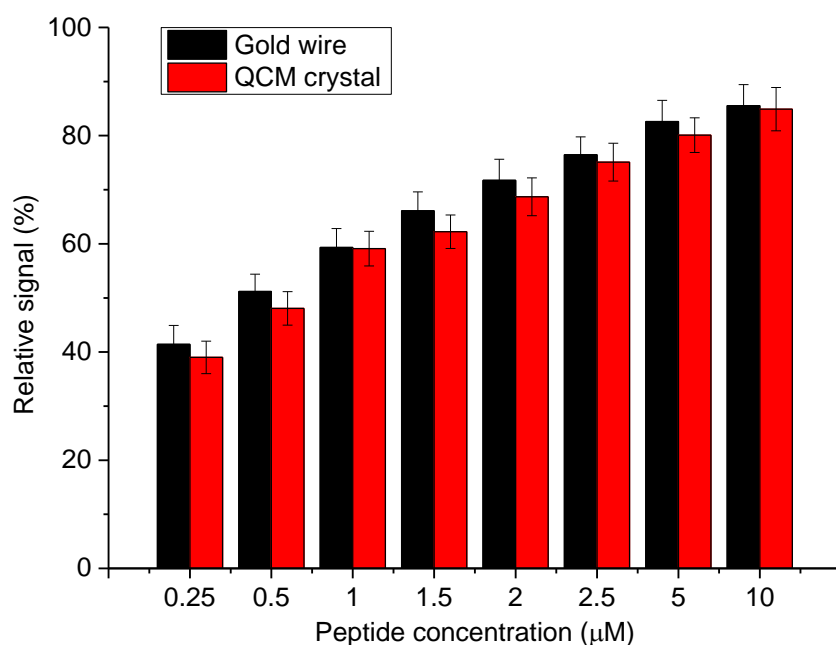


Figure S1. The comparative rebinding studies with the MIPs formed on gold wires or QCM crystals. The MIPs were prepared using the same polymerization cycle and template removal conditions and then exposed to the different concentrations of the NSE derived peptide.

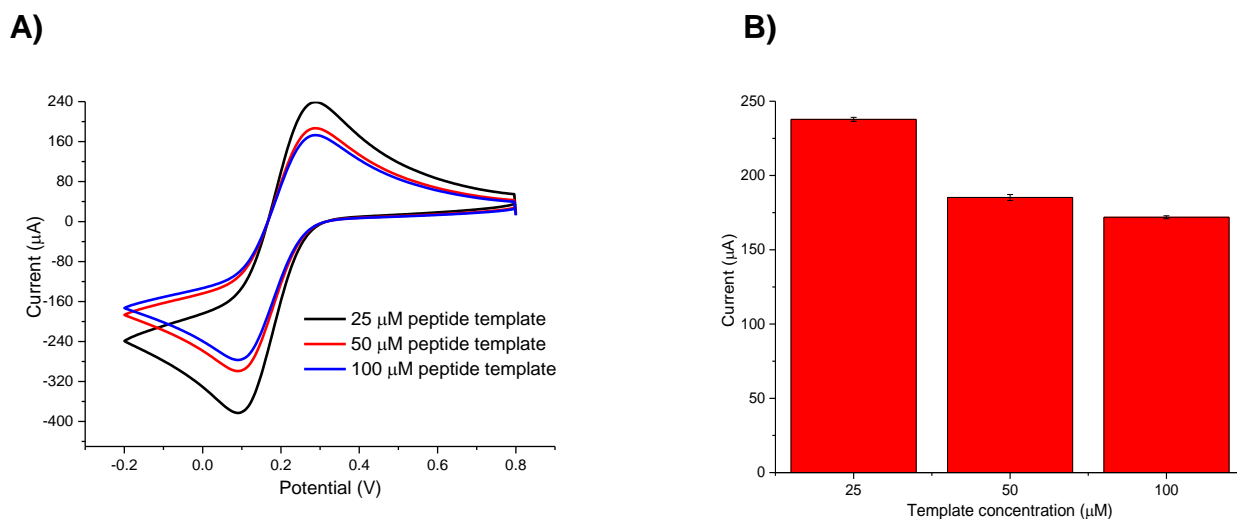


Figure S2. Optimization of template concentration. A) Cyclic voltammograms recorded in 10 mM $K_3[Fe(CN)_6]$ containing 100 mM KCl for the attachment of the peptide template at three concentrations (25 μM , 50 μM , 100 μM). B) Overall results of the template adsorption on the gold surface with standard deviation of the data (n=3).

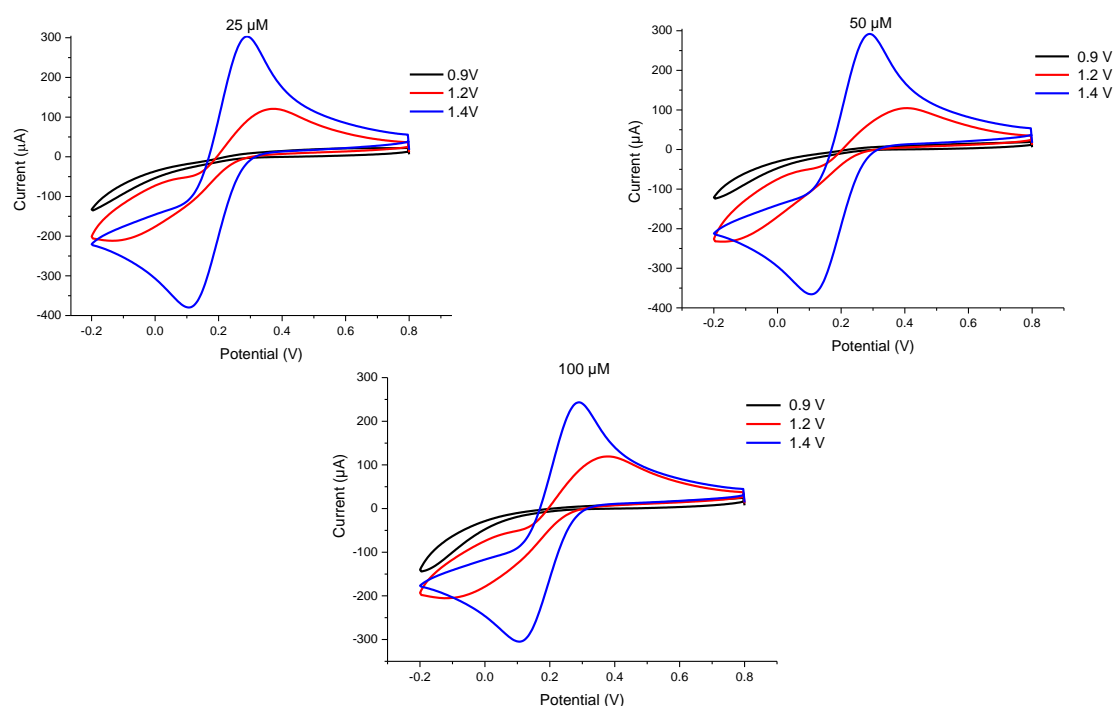


Figure S3. Optimization of template removal. Cyclic voltammograms recorded in 10 mM $K_3[Fe(CN)_6]$ containing 100 mM KCl for the removal of the template at three different concentrations (25, 50 and 100 μM) by applying three different anodic potentials (0.9, 1.2 and 1.4 V). The results obtained at 1.4 V confirmed the complete template removal for 25 and 50 μM of the pre-adsorbed template as the bare wire generates a peak signal of 290 μA . All measurements were performed under exactly same conditions. Each voltammogram represents average results of three measurements.

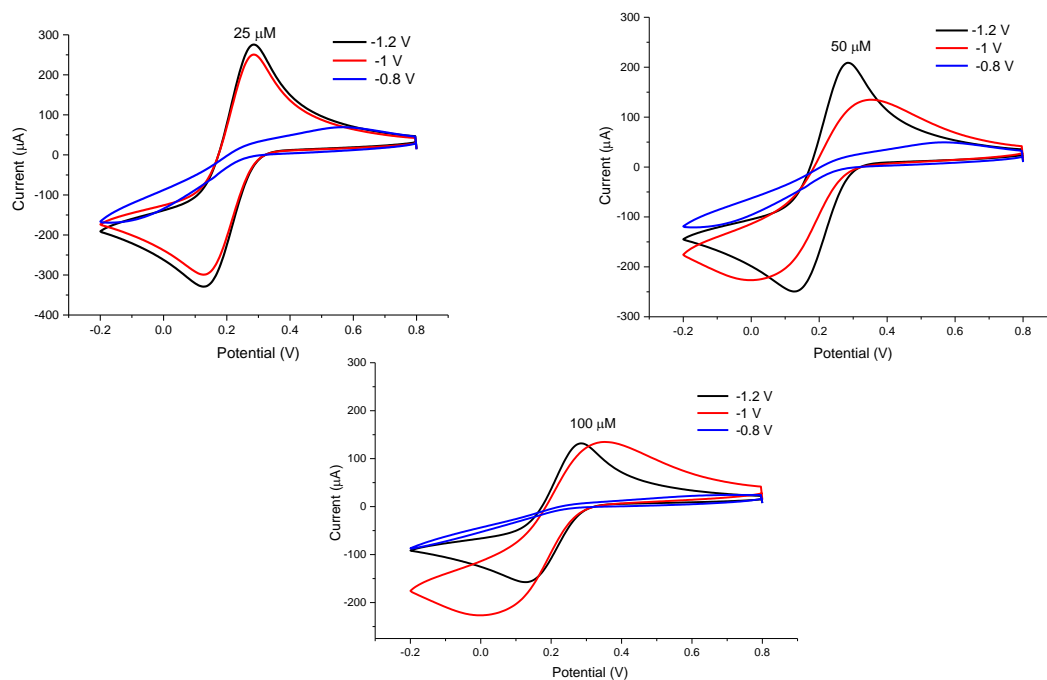


Figure S4. Optimization of template removal. Cyclic voltammograms recorded in 10 mM $K_3[Fe(CN)_6]$ containing 100 mM KCl for the removal of the template at three different concentrations (25, 50 and 100 μM) by applying three different cathodic potentials (-1.2, -1 and -0.8 V). The potential application only at -1.2 V could remove the template to some extent at 25 and 50 μM concentrations. Reference point: the peak signal of bare surface (290 μA). All measurements were performed under exactly same conditions. Each voltammogram represents average results of three measurements.

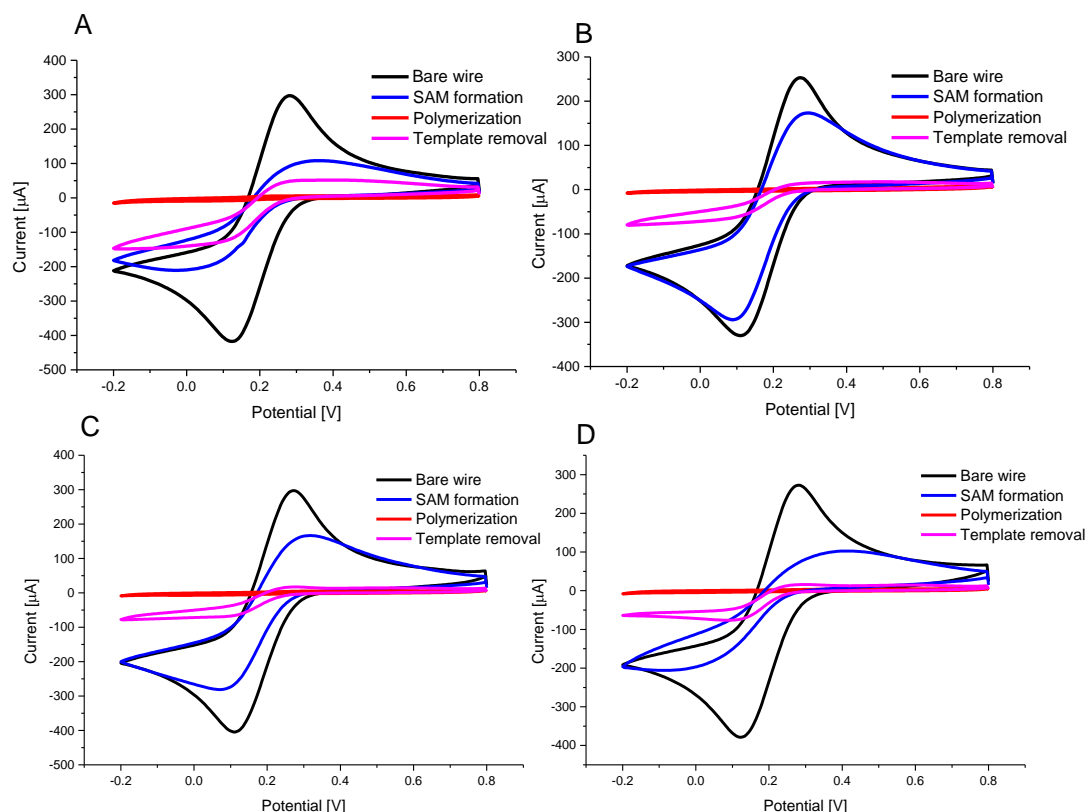


Figure S5. Characterization of molecular imprinting process from bare electrode surface to the end of template removal. Optimization of functional monomer concentration and polymerization cycle under pre-determined optimal template concentration (50 μM) and template removal (-1.2 V potential application) conditions. MIPs were prepared with a 0.5 mM (A, B) or 1 mM (C, D) concentration of functional monomer (scopoletin). Polymerization was achieved by 25 (A, C) or 50 electropolymerization cycles (B, D). Each cyclic voltammogram represents an average of three voltammograms recorded in redox marker solution. The potential application at -1.2 V was tested in whole imprinting process as it could remove the pre-adsorbed templates at 25 and 50 μM to some extent in preliminary optimization studies. As expected, the template removal from the polymer network could be observed at a low level only in case of using a 0.5 mM concentration of the functional monomer and 25 electropolymerization cycles (A). In all other conditions (B, C, D) the template removal was drastically low.

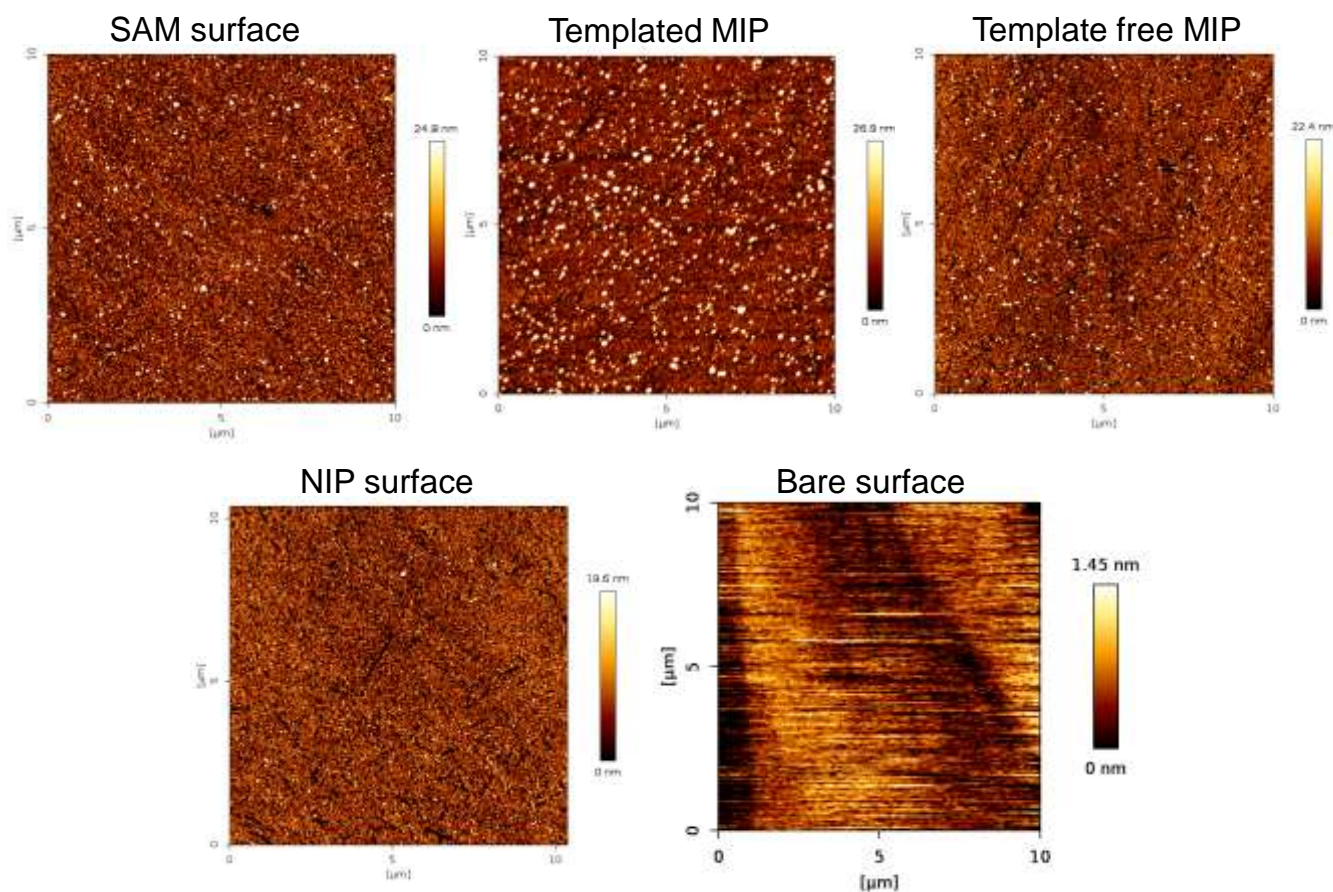


Figure S6. The AFM characterization of molecular imprinting process. The AFM 2D height images of bare gold surface (height value: 1.45 nm), SAM surface (the template adsorbed surface, height value: 24.8), templated MIP (height value: 26.9 nm), template free MIP (height value: 22.4 nm), and NIP surface (height value: 19.6 nm).

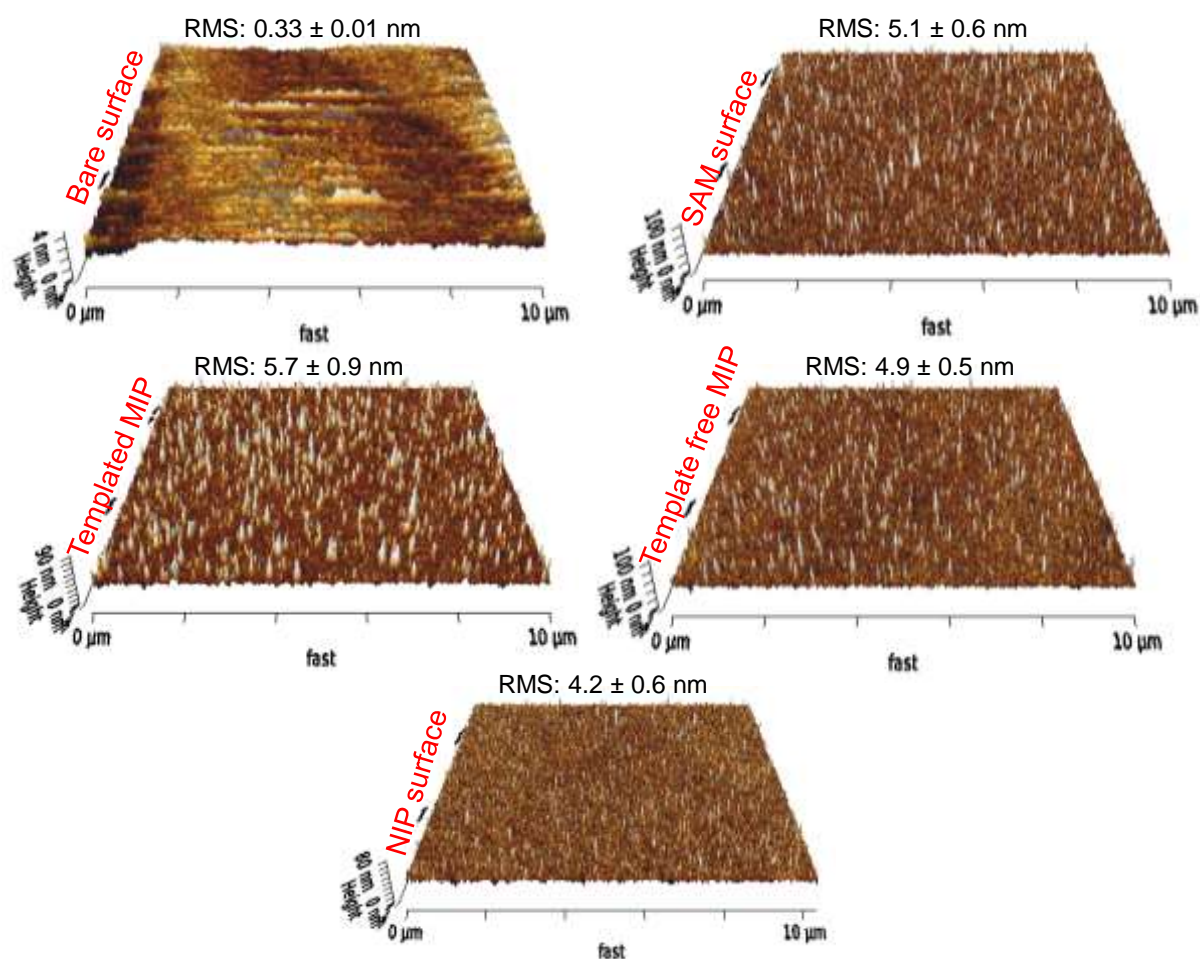


Figure S7. The AFM characterization of molecular imprinting process. The AFM 3D surface topology images of bare gold surface, SAM surface (the template adsorbed surface), templated MIP, template free MIP, and NIP surface along with the RMS value of each surface. The RMS results are average of 10 cross-sectional data.

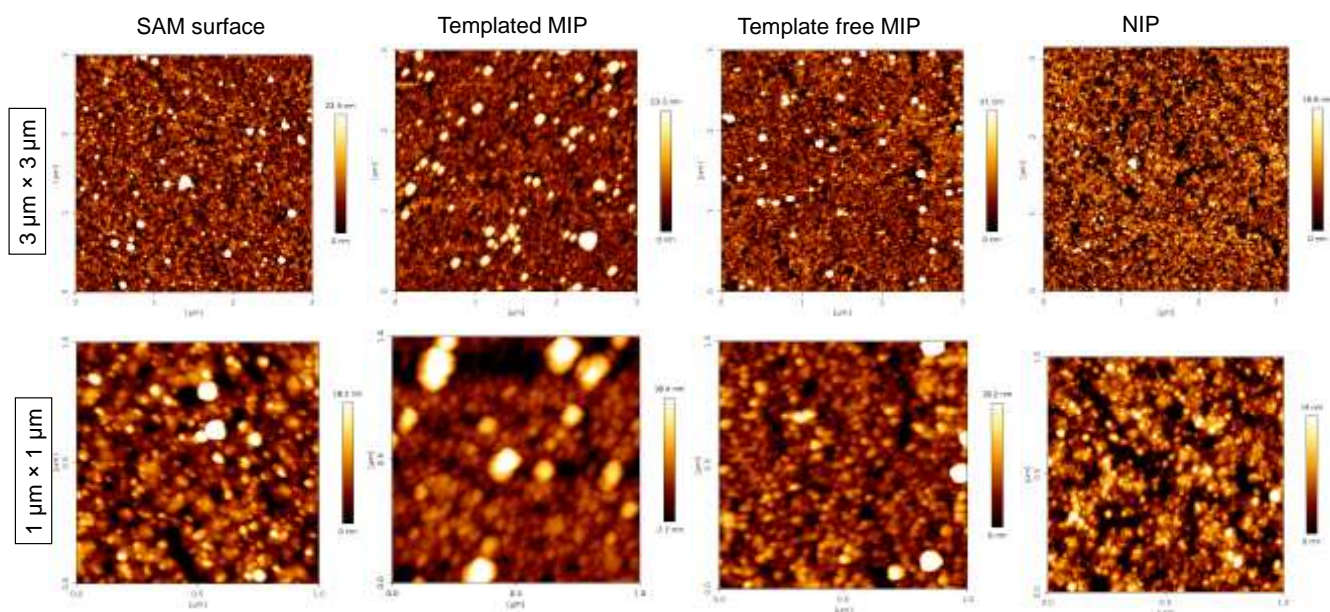


Figure S8. The AFM 2D height images at 3 μm^2 (upper row) and 1 μm^2 (lower row) scanning areas.

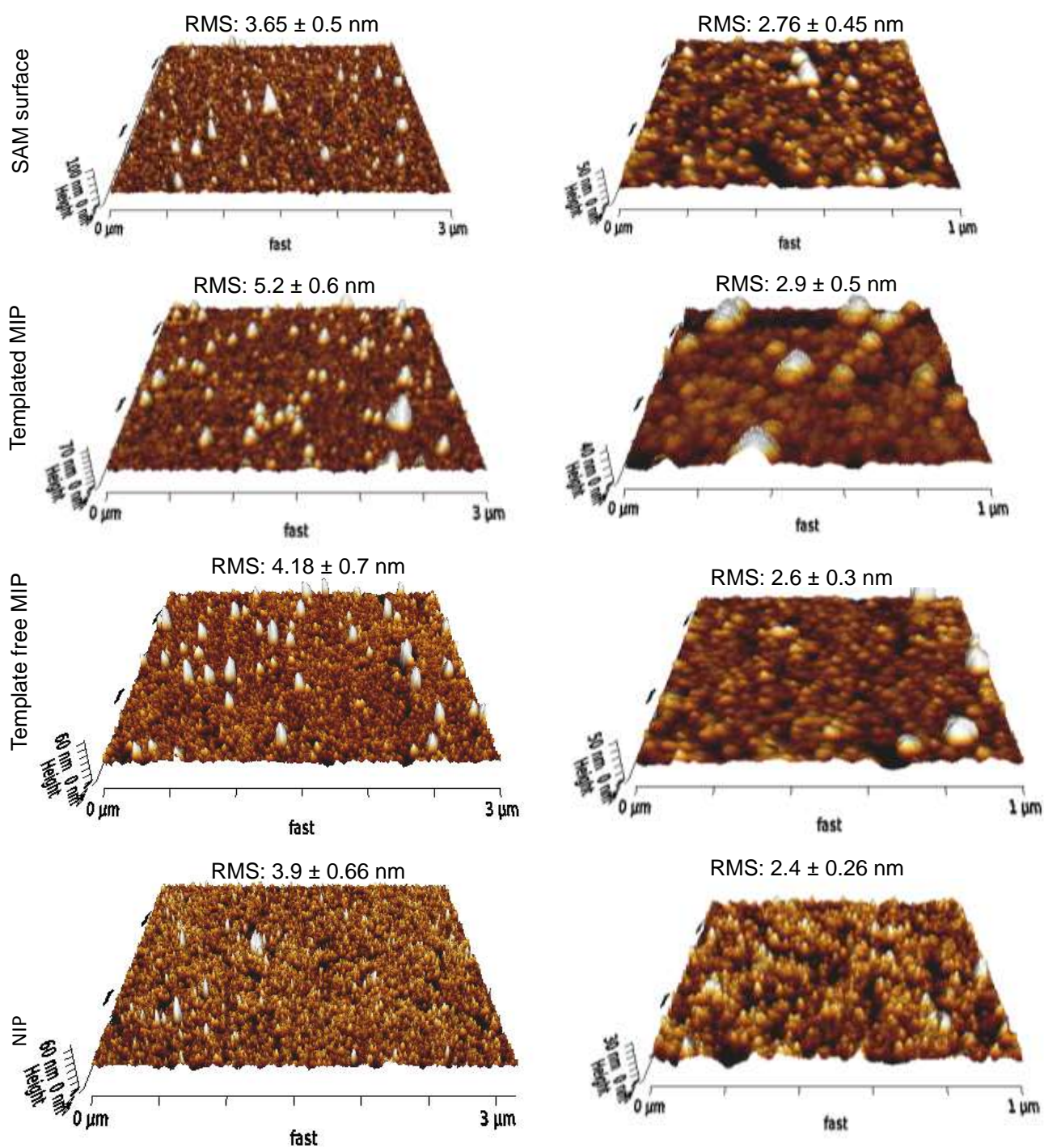


Figure S9. The AFM 3D surface topography images at 3 μm^2 (left) and 1 μm^2 (right) scanning areas.

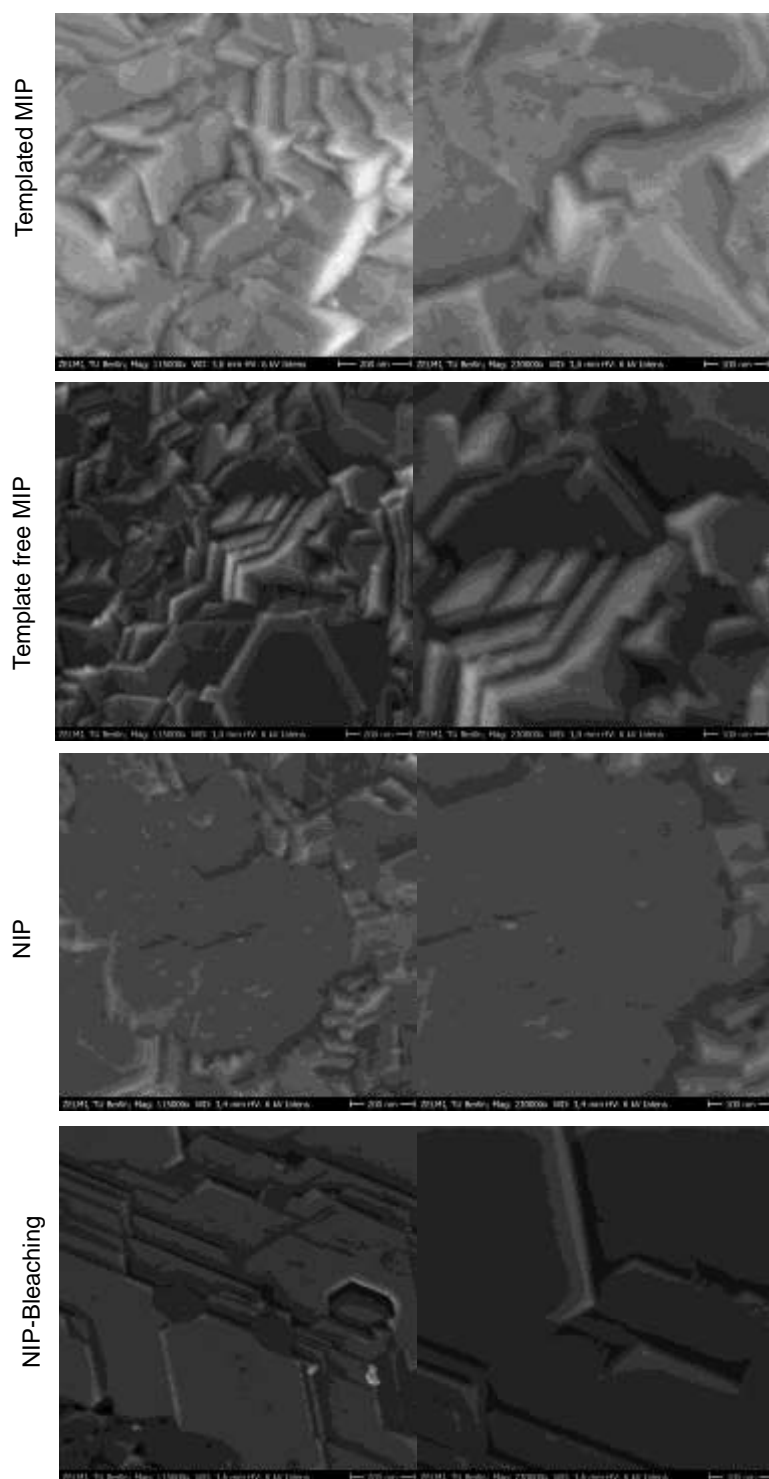


Figure S10. The SEM characterization of molecular imprinting process at 11500x (left column) and 23000x (right column) magnifications. The polymer film following electrodeposition can be seen as a thin film enveloping the gold surface. The existence of dark macrodomains with an average size of 208 ± 85 nm can be attributed to the template removal process. Application of the template removal conditions does not cause the formation of macrodomains in the NIP as these pores form due to the desorption of epitopes from the gold surface. The bleaching of NIP however, does cause the polymer film to peel from the surface to an extent which is represented by small dots of 39 ± 15 nm diameter.

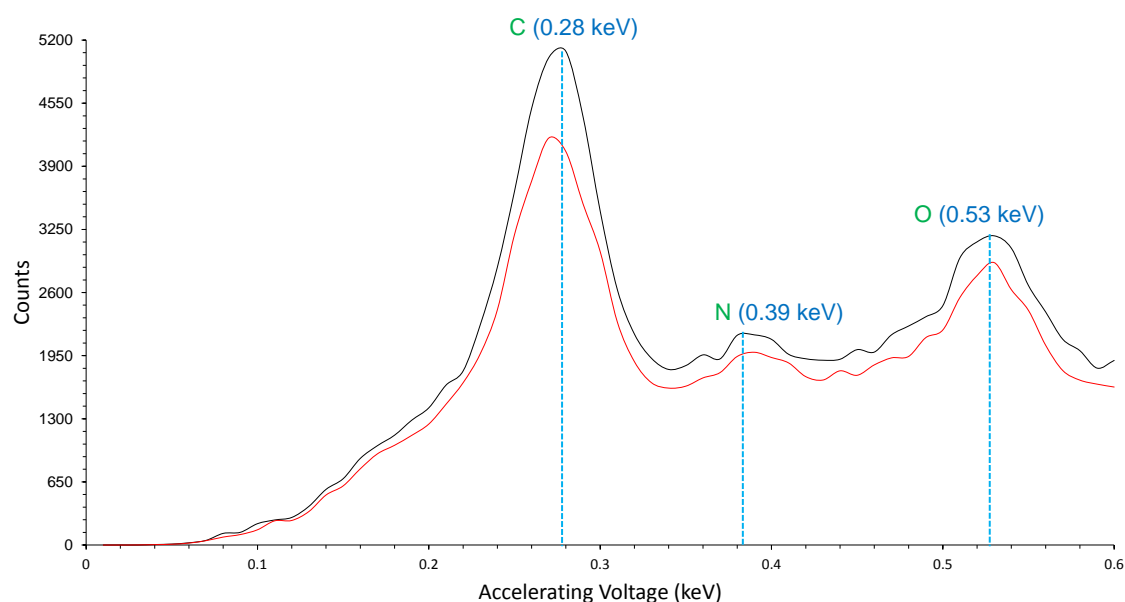


Figure S11. The EDX spectrum of MIP before and after template removal. C, N and O, the reduction in the number of atoms of other non metals can be a helpful tool in analysing the presence of template molecules. The low energy peaks were all located between 0.0 – 0.6 keV. As amino acids have a large number of carbon atoms, the change in the C atom peaks (0.28 keV) was larger than that of N (0.39 keV) and O (0.53 keV). The MIP with epitopes still embedded within displayed 5083 counts of C atoms. In the absence of epitopes, this number sharply reduced to 4197 corresponding to a 17% decrement. In comparison, count of N atoms reduced by 8.1 % and similar alteration was observed in case of O atoms (8.7%).

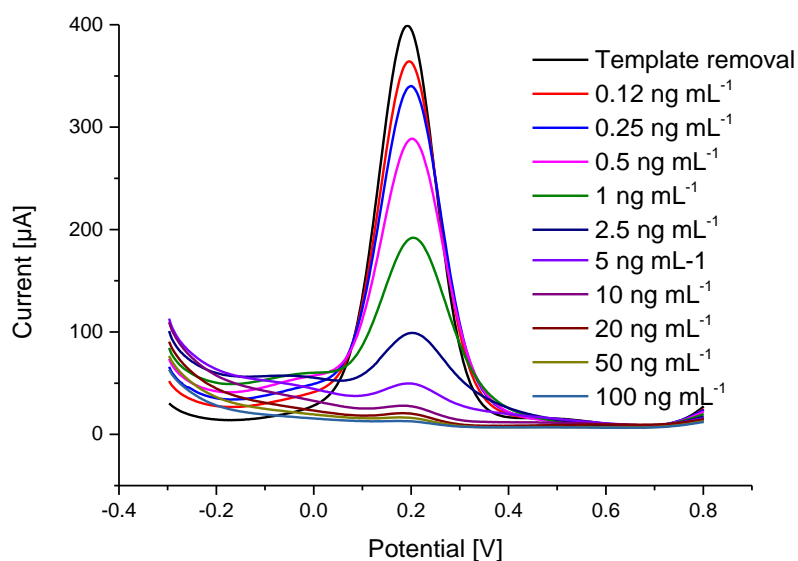


Figure S12. Square wave voltammograms showing the NSE biomarker detection using the MIP sensor in the concentration range of 0.12–100 ng mL⁻¹. Measurements were taken in redox marker solution after incubating each protein sample for 30 min with the MIP electrode. The signal suppression is proportional to the concentration of protein loaded onto MIP surface. The measurement for the template removal acts as the reference point to ensure the rebinding process.

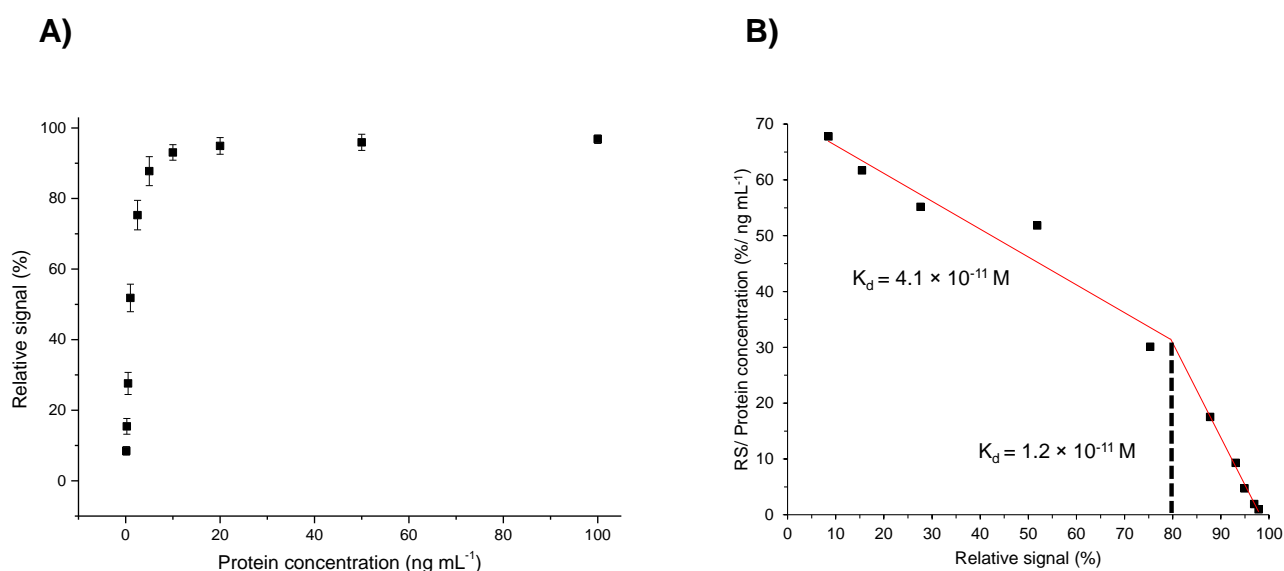


Figure S13. A) Concentration-dependent protein detection using the MIP sensor in a range from 0.12 to 100 ng mL⁻¹. B) The Scatchard plot for affinity determination of the sensor for NSE protein in buffer.

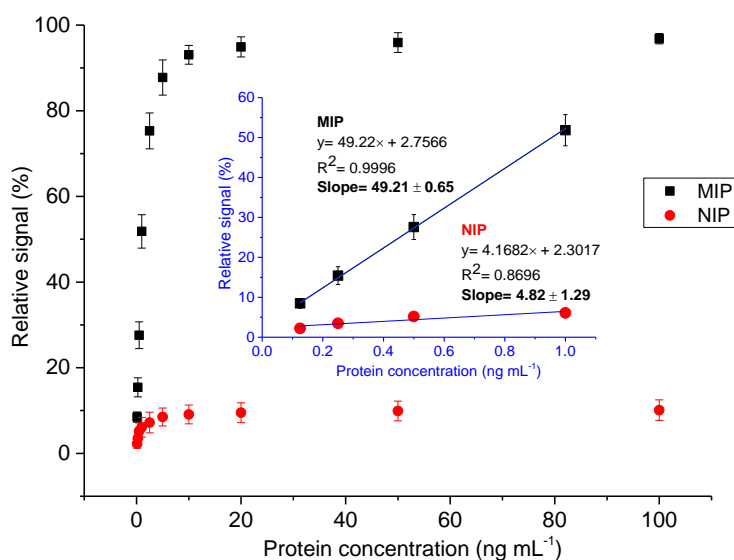


Figure S14. Comparison of affinity binding between the MIP and the NIP in the concentration range of 0.12–100 ng mL⁻¹ for the NSE protein. Imprinting factor was calculated as 9 in the entire investigation range by dividing the average signals of MIP and NIP. Inset: the IF was determined as 10 based on the slope ratio of the MIP and NIP assays in a linear range.

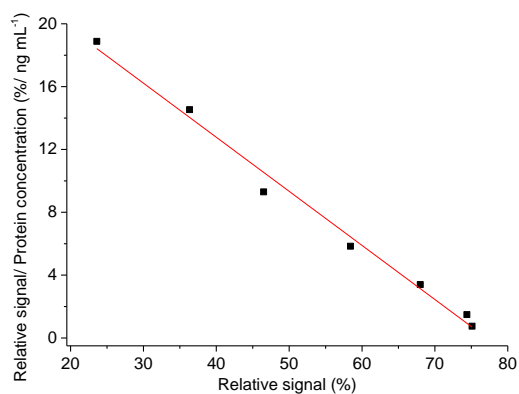


Figure 15. The Scatchard plot for affinity determination of the sensor for NSE protein in serum, $K_d = 6.4 \times 10^{-11} \text{M}$.